Article ID: WMC004995 ISSN 2046-1690

Significant changes detection in the follow-up of Retinal Pathologies through computer analysis of Optical Coherence Tomgraphy

Peer review status:
No

Corresponding Author:
Prof. Maurizio Baroni,
assistant professor, Department of Information Engineering, via S.Marta 3, 50139 - Italy

Submitting Author:
Prof. Maurizio Baroni,
assistant professor, Department of Information Engineering, via S.Marta 3, 50139 - Italy

Other Authors:
Dr. Francesco Matassoni,
Biomedical Engineer, Department of Information Engineering, Firenze, via S.Marta 3 - Italy

Article ID: WMC004995

Article Type: Research articles

Submitted on:23-Oct-2015, 11:54:02 AM GMT **Published on:** 24-Oct-2015, 01:37:10 PM GMT

Article URL: http://www.webmedcentral.com/article_view/4995

Subject Categories:BIOMEDICAL ENGINEERING

Keywords: Retinal pathology, Optical Coherence Tomograhy, Texture analysis

How to cite the article: Baroni M, Matassoni F. Significant changes detection in the follow-up of Retinal Pathologies through computer analysis of Optical Coherence Tomgraphy. WebmedCentral BIOMEDICAL ENGINEERING 2015;6(10):WMC004995

Source(s) of Funding:

This work was supported by a research fund of Florence University.

Competing Interests:

The authors have no financial or personal relationships with other people or organizations that could inappropriately influence this work. No Ethical Approval is required.

Significant changes detection in the follow-up of Retinal Pathologies through computer analysis of Optical Coherence Tomgraphy

Author(s): Baroni M, Matassoni F

Abstract

Recently, Optical Coherence Tomograhy (OCT) is widely used to investigate retinal pathologies.Quantitative methods are needed to support qualitative evaluation carried on by medical specialists. Besides retinal thickness measurement, tomographic imaging allows to study macula morphology and tissue structure of retinal cellular layers. Pathological conditions are expected to alter this tissue appearance. Therefore, in the present work, image texture analysis is used to differenziate normal retinas from pathological ones as well as to detect significant changes in follow-up studies. Classical second order statistics, i.e. co-occurrence matrices, and a recent method, known as Local Binary Pattern (LBP), are applied to 25 normal subjects and to 34 patients, affected by vitreo-retinal interface traction syndrome or by retinal edema with various etiology. Both methods have shown a good capability to discriminate between normal and pathoplogical images: a few measured features exhibit signficant differences ($p< 0.05$) in inner retina, with a strong stability on varying method parameters. Then, a follow-up study was performed: 16 pairs of OCT images of pathological eyes, captured at different times, were selected out of a wider database of consecutive clinical examinations so that they were centered on the fovea, well aligned horizontally and without acquisition artifacts. Details of methods are discussed in the text. Results show a good agreement between clinical findings and the outcomes of co-occurrence, LBP and thickness analysis. Of particular interest is the analysis of critical pixels based on LBP, that allows to follow the pahology evolution in a simple, quantitative way.

Introduction

Since the mid of 1990 years, the study of retina and its disease [1] can be performed also with Optical Coherence Tomography (OCT): it is a non-invasive high resolution, high sensitivity, digital technique [2,3] that uses interference patterns of low coherence infrared light for imaging subsurface tissue structure and that is particularly suited for transparent tissue such as the eye. Given its micron resolution, OCT tomgrams show sections of retina (illustration 1) that, before, could be observed only in vitro, with microscopy (illustration 2). Though the signal captured by the OCT scanner is monochromatic, images are shown in pseudo-color for contrast enhancement and display convenience. However, OCT digital image processing works on the original gray level images. Generally, OCT images are evaluated in a qualitative way [4], thanks to the experience accumulated over the years by specialists, with the only exception of measurement of retinal thickness, that has an inverse relationship with visual acuity. With all probability, we can accept the hypothesis that disease changes the structure of the affected retinal tissue. In particular, it is expected that this will change the appearance of tissue (the so-called texture) besides morphology of fovea and of tissue layers. Therefore in this papers two known methods, developed in the field of digital image analysis [5], were adopted to investigate whether and how disease affects image texture: Gray Level Co-occurrence Matrices (GLCM) [6,7] and Local Binary Pattern (LBP) [8,9]. The measured values for GLCM were five Haralick indeces, as already well known in literature [10]: entropy, contrast, correlation, energy, homogeneity. The measured values for LBP were LBP decimal code and LBP contrast. Both methods need to choose some parameters, such as the size of Region of Interest (ROI) where computation must be done. So, the stability of results on varying method parameters will be carefully considered. Moreover, morphology of foveal area was quantified with a new thickness index. Methods have been implemented in our laboratory with PCs and Matlab development enviroment, licenced to Florence University.

As a first application, two groups of retinal OCT images (25 normal and 34 pathological eyes) were used to test the diagnostic capability. Secondly, a follow-up study was performed on another group of 16 eyes, which were examined by OCT at two different times during medical treatment. In both applications, the results of GLCM, LBP and foveal index are in agreement, with minor discrepancies, and this gives a

greater consistency to the conclusions. It is shown how the results, in particular those of LBP, are in agreement also with standard retinal thickness analysis. Finally, it was revealed a peculiar behavior of the LBP, which could eventually allows the segmentation of potential retinal edema.

Materials & Methods

Patient Data

A StratusOCT scanner (Carl Zeiss Meditec, California USA), at Department of Surgical Oto-Neuro-Ophthalmology Sciences, University of Florence, was used to perform OCT imaging.

Horizontal B-scans of 6 mm length, across fovea, were acquired with the regular line protocol, choosing the OCT image where the foveal area is better delineated, according to the fundus image provided by the OCT instrument. Twentyfive normal images and 34 pathological images were recruited for diagnostic study, together with 16 pairs of OCT images of pathological eyes, captured at different times: these were selected out of a wider database of consecutive clinical examinations so that they were centered on the fovea, well aligned horizontally and without acquisition artifacts. In this way, the follow-up study is made easier. However, the method does not lose its generality, because image registration may be performed as a pre-processing step.

In our casuistry, the Propanololo therapy was used in follow-up study and the following retinal disease were found: Macular Pucker, Vein Thrombosis, AgeRelated Macular Degeneration and Diabetic Retinopathy.

To make computer analysis of retina, for each OCT images three main contours were digitized by ophthalmologists, even though there are software able to make image segmentation of retina in its varoius layers [11,12]. The first contour (illustration 3) represents the vitreo-retina interface; the second one divides the external plessiform layer from the external nuclear layer, i.e. it is the interface between inner and outer retina; the third contour is the external limiting membrane. In fact, the study focuses itself on two parts of retina, the inner layers and the outer photoreceptor layer, as well as on full thickness retina. However, some computation (see later) has to be made on ROIs of each retinal part. In illustration3, five ROIs, centered on fovea, are delimited by green vertical straight segments.

Retina thickness and Fovea shape index

In digital OCT images it is possible to measure layer thickness, by using the distance between the aforementioned three contours. This is the standard analysis [13], available in the software implemented on commercial OCT scanners. In fact, most ocular diseases alter the retinal thickness, often causing the disappearence of the typical foveal depression. So that it is essential to evaluate foveal morphology, too, besides its thickness.

Therefore, the following new fovea shape index, It, is devised:

$$It = 2\,t2 / (t1 + t3)$$

where t1 is the average thickness in the ROIs on the left of fovea, t2 is the average thickness in the foveal region, and t3 is the same in the ROIs on the right of fovea.

This shape index is the ratio between the central thickness and the average of lateral thickness: it is greater than 1 if foveal depression is altered; it is less than 1 when fovea shows a subsidence, as in normal eyes; it is near null in case of macular holes.

Usually, thickness is measured in pixel: it does not matter to express thickness in microns, because we shall evaluate its difference between normals and patients, as well as thickness changes over time.

Texture

As already said, we are interested to make a quantitative description of the so called image texture [5], defined as any geometric, repetive arrangement of image gray levels.

In fact, in retinal OCT images, both cellular layers and neural fibers are visible as ordered sequences of fine grained structures, even if their interpretation is complicated by the presence of speckle noise [14]. It does not exist a unique method for texture description. The human visual system recognizes different textures in a qualitative way, as coarse, fine, grained, thread-like, ordered, casual, etc. Quantitative appoaches mark the difference between macro-structures, i.e. regular, coarse primitives (texels), and microstructures, i.e. casual, thin arrangements related to few pixels. This latter is the case of retinal OCT images, where a statistical approach to texture description is particularly suitable, even if there exist other methods [5,8] based on correlation, spectral analysis, multiscale spatial filtering, etc..

Gray Level Cooccurence Matrix (GLCM)

The most common class of texture description uses second order statistcs of image gray levels, i.e. it is based on the relationships of groups of two pixels. A simple method builds histograms of absolute gray

level differences between neighbouring pixels, e.g. considering four neighbour or eight neighbours in 3x3 windows. A more general method extends the neighborhood over 3x3, leading to the well known formulation of co-occurrence matrices (GLCM): for all possible pairs of pixels (a, b) at a given distance d=(dx,dy), the number of times that they have gray levels Ga and Gb, respectively, is computed and saved in the corresponding element of GLCM(Ga, Gb). If one divides these counts by the number N of the pixel pairs, at the distance d, an approximation of joined probabililty of the gray levels of pixel a and b is obtained:

GLCM(Ga, Gb, d) = # (Ga, Gb) / N » p(a-b, Ga, Gb) = p(a, b, Ga, Gb)

where the symbol # stands for “number of”; the last equality holds with the assumption that this probability distribution is stationary (not dependent by spatial location). A different co-occurrence matrix is obtained for each possible distance value, that mus be small (d=1,2, 3) because greater distances make the pixel pairs uncorrelated, leading to information loss. GLCMs are always square with dimension m x m, where m is the number of gray levels; they are asymmetric but it is always possible to make them symmetrical summing their transposed matrix. GLCMs are generally computed in rectangular or square regions (ROI) that are smaller than the entire image. Unfortunately, sometimes there are problems of redundance and instability, because the number of matrix elements is greater than the number of pixel pairs used for estimation; moreover, GLCMs are sparse for the limited gray level variability in a ROI. Other properties of GLCM are discussed in literature [5-7], however, the following parameters were tested in our application, in order to avoid the aforementioned problems and to obtain the best results: the distance value (d=1 and 2); the distance orientation (horizontal, vertical, not diagonal);the number of gray levels (m=256, 64, 16); only symmetrical matrices.

As regards the ROI dimensions, the particular arrangement of OCT retinal images must be considered. In illustrations 1-3, one can see that cellular layers lie in horizontal direction and are delimited vertically by three contours; so, only the horizontal dimension of ROIs, D, remains to be chosen, e.g. D values could be between 1/20 and 1/100 of OCT image width. The exact value depends on a compromise among three reasons: the stationarity hypothesis (not valid if an entire retinal layers was considered as ROI), the necessity of including sufficient data to avoid meaningless, sparse matrix and the opportunity of extracting localized information on retinal physio-pathology. Besides, another criterion to select the D value is that the number of ROIs must be odd, in order to have a central ROI for fovea.Finally, it is worth noting that GLCM computation ignores pixel pairs in a rectangular ROI if either of the pixels is outside the current retinal layers: in those particular pixels the value of NaN is used.For a more compact description of GLCMs, only five out of 30 Haralick features (entropy, contrast, correlation, energy, homogeneity) were computed, as they are independent each other.

Local Binary Pattern (LBP)

Another approach to texture analysis was developed [8] both to limit the computation complexity and to overcome the problem of invariance. In fact, texture visual appearance depends on variations in gray-levels, orientation and scale. To this aim a new operator, called Local Binary Pattern (LBP), is defined on a circular neighbourhood of each pixel (illustration 4). How one can see, the gray level of the central pixel thresholds the levels of the other pixels, in order to compute a contrast value (C) as well as a binary code (LBP). Weighting the binary digits with powers of two allows LBP to be turned into decimal. In the illustrated example, a 3x3 windows and np=8 neighbours are used: however, the neighbourhood can be wider, on condition that only the pixels belonging to its perimeter are considered.

Invariance to monotonic transformations of gray-scale is achieved by subtracting the central pixel level and by considering only the signs of these differences (in illustration 4: the thresholded values are 1 for positive differences and 0 for negative ones).

To warrant also rotation invariance, the lowest LBP code is considered among all the np possible rotations with different initial position. To the same task, the contrast value is computed as gray level variance in the neighbourhood.

Scale invariance can be achieved by using multiscale LBP. It is obtained by summing a few LBP codes with different radius, even if the number of neighbouring pixels, np, does not change (the perimeters is sampled with the same equidistant points). In multiscale LBP, the contrast value becomes meaningless.

It is possible to construct histograms of LBP codes, but to reduce dimensionality and noise, the local patterns that are sparse, non-uniform, can be collapased to a unique value. In [8] LBP patterns are uniform if they have at most two transitions from 1 to 0 or from 0 to 1, in the circular neighbourhood; they are assigned labels between 0 and np. Therefore, the other patterns, nonuniform, are assigned the label

np+1. This operation must be made before the trasformation of binary to decimal code (by multiplication with the corresponding weights, illustration 4), as well as before the rotation invariance transformation.

Further discussion on LBP can be found for example in [9].

In our application, inner and outer retina have to be analysed. Again, since the retinal layers are arranged horizontally in OCT images, the neighborouhoods for LBP calculation can be rectangular or square (not yet circular) regions. Therefore, in our experiments, the LBP parameters to be chosen were the horizontal and vertical dimensions of neighbourhoods, from 3x3 to 7x7.

In illustration 5, some multiscale LBP neighbourhoods are shown. Of course, the neighbourhoods with some pixel lying outside the current retinal layer, are neglected in LBP computations.

Statistical Analysis

Statistically signficant differences were investigared between normal and pathological images by using unpaired Student's t-test. For the features measured in normal images, the 95% range (mean ± 2 sigma) was computed and used in the follow up study.

Also in the latter study, statistical differences between OCT images captured before and after medical treatment were investigated with paired Student's t-test. To make the results independent from hypotheses of t-test, also a non parametric test was used, Wilcoxon rank-sum test.

In all the investigations a significance level of p=5% was chosen.

Results

The first results regard whether the implemented methods succeed to distinguish between healthy and pathological retinal OCT images. Also the sensitivity of the methods towards variations of their input parameters were investigated.

For Gray Level Co-occurrence Matrix analysis, five Haralick features were measured and found statistically different between the two image groups. In particular, they do not vary in a significant way by changing the distance offsets, d=(dx, dy), such as (0,1), (0,2), (1,0), (2,0). By varying the gray level number used in calculation, m=(256, 64, 16), its reduction does not allow better results, so the original 256 gray levels are considered. The number of tested ROIs were Nroi=45, 29, 15 or 5, which correspond to about D=15, 25, 45 or 138 pixel width per region, respectively. Illustration 6 shows the best results, obtained for five ROIs of full thikness retina, with m=256 and offset (0,2). Normal ranges (mean value ± 2 standard deviation) of five Haralick features, in 5 ROI and in full retina, are reported for documentation. Standard deviations are very small in normal eyes, as well as they are higher in patients.

In the comparison between normal versus pathological groups, a significant difference (marked in yellow) was found only for two out of five features: entropy and energy (even if also correlation gives a low p=5,8%). In the last row of table, also the comparison accuracy is reported. For brevity, the other results are not shown as tables; instead, they are illustrated in the following. In particular, results with greater values of Nroi confirm the discrimination capability of entropy and energy, even if only energy remains statistically different (p< 5%) for Nroi=29 and 45.

By restricting the GLCM analysis in inner retina, three Haralick features are significantly different: also correlation (p=4.1%), besides entropy (p=0.6%) and energy (p=0.4%). On the contrary, no Haralick feature exhibits significant differences (p=9% up to 63%) in outer retina.

Local Binary Pattern analysis confirms both the stability on varying the input parameters and the significant difference between normal and pathological groups only in inner retina. Such a difference gives good p-values (< 5%) with 3x3, 5x3, 7x3, 5x5, 7x5 or 7x7 neighborouhoods only for LBP code, in inner reina. As before, the best results are shown as a table (illustration 7). Contrast and LBP code cannot distinguish texture of outer retina between normal and pathological groups. Results become better with multiscale LBP analysis (p< 1%), again only in inner retina, showing the largest difference (p< 0.001%) with 3x3 and 7x7 neighbourhood combination (illustration 8). Interestingly, both GLCM and LBP do not distinguish the outer retina texture between our normal and pathological groups, perhaps because the pathologies involved do not alter the photoreceptor layers.

A further analysis was performed by decomposing the inner retina into its three main components: gangliar cells and inner neural fibers (CGL+IPL), bipolar cells (INL), and outer plessiform layer (OPL). Again, a significant difference (p< 2%) was found with multiscale LBP (3x3 and 7x7), the first sublayer being the worst (p< 0.3%). On the other hand, also multiscale LBP analysis on full thickness retina showed a significant difference between the two groups (p=3.05%), even if it is worser than inner retina

for the confounding contribution of outer retina. According to GLCM anlaysis, LBP code exhibits a higher standard deviation in patients (96.99 ± 7.14) with respect to normal retina LBP (91.7 ± 4.9).

In the follow-up study, two retinal OCT images of 16 pathological eyes, captured at different times, during medical therapy, are available and are called pre and post images, respectively. They must be evaluated to understand whether there was an improvement or not. Visual inspection by experienced specialists is taken as gold standard: in particular, he/she is asked whether both edema and fovea morphology became better, worser or they remain the same (last columns of illustration 9).

Texture and thickness analyses are applied to identify and quantify temporal changes, in the same way that they were used to distinguish between normal and pathological eyes. At this regard, the results of statistical tests on GLCM features, as measured on five ROI in every pairs of the given 16 cases, are shown in illustration 9 (GLCM p% column), for full thickness retina analysis (similar results were obtained for inner and outer retina). As one can see there are three out of sixteen results that do not agree with gold standard, giving about 81% accuracy.

As an alternative, also normal ranges of the same GLCM features, in every ROI (illustration 6), could be used to identify changes (first column of illustration 9). For example, no change is detected in the first case, because all (or the majority of) the features remain within their normal range or they remain outside it. Accordingly, the second case improved, as all the feature values, which were outside, turned back inside their normal ranges. It is worth noting that this alternative GLCM evaluation allows also to know where improvement or worsening happened (e.g. in fovea or in a lateral region), even if with a worser accuracy (75% vs. 81%).

Statistical tests of LBP analysis, based on paired ROIs, gave poor results, with only nine results, out of sixteen, that agree with gold standard (not shown in illustration 9): in particular, more changes are detected in outer retina (11 changes with respect to only 3 in inner retina). In this follow up study, it seems that LBP results are not as valid as in the preceding study. In fact, while the GLCM method evaluates wide regions of pixels, this method averages LBP values based on small neighbourhoods of each pixels. Therefore, we tried an alternative method that uses normal ranges of LBP values in full thickness retina, in a similar way as used before, in GLCM evaluation. Specifically, individual Local Binary Patterns (LBP) are considered as pathological values, and labeled as critical pixels, if they are higher than their normal range (91.7 ± 4.9 *2), i.e. greater than 101,5. The spatial distribution of these critical pixels tend to accumulate inside edema, as shown for two cases of the follow-up study in illustrations 10 and 11.

Therefore, it is reasonable to evaluate the severity of a given retinopathy by simply counting the number, c, of critical pixels present in the image. If the size of edema decreases, also critical pixels decrease. Consequently, the difference between the number of pixels in the pre and post images (Dc) must be positive, in the event of improved conditions; negative, in case of worsening.

These LBP results were compared with retinal thickness values, measured and averaged on the same images: accordingly, the thickness difference (Dt) between pre and post mages is positive in case of improvement, negative, in case of worsening. As one can see in illustration 9, there was agreement in 15 out of 16 cases. Also comparison with gold standard (the last column but one in illustration 9) gives only two disagreement for Dc and one for Dt.

Finally, as far as fovea morphology is concerned, the difference in foveal shape index (DIt) agrees with gold standard (last column of illustration 9) in 15 out of 16 cases, with a 93.75% accuracy.

Discussion

Detection of changes in retinal images is a valuable resource in the follow-up of evolving retinopathies, such as diabetic retinopathy. When compared with color fundus imaging and fluorescein angiography, OCT has demonstrated [4] superior capabilities to aid in the diagnosis of macular edema, able also to distinguish between retinal edema and serous detachment.

Though methods for change detection in fundus images have been reported, e.g. [15], quantitative tools for such change detection is not yet available for OCT images, as thickness measurement cannot identify all the possible variations, e.g. in case of co-existing pathological conditions.

This work has shown that there exist a significant correlation between retinopathy and texture of retinal OCT images: both GLCM and LBP analysis can distinguish between normal and pathological retinas, also with a good robustness against image noise and methodological parameter variations. The GLCM method already gave good results in OCT texture analysis of macular pucker [12]. In the present work the multiscale LBP method exhibits the best results.

This was introduced recently and we have found only one study that uses LBP in the field of OCT retinal images [16]. On the other hand, LBP has the three important properties of multiscale analysis, invariance to rotations and to monotonic gray scale variations.

Also in the follow-up study both texture methods have shown good results, in agreement with thickness analysis and qualitative evaluation. Problems arise when the central ROI is not algned with fovea. For this reason the greatest ROI width was chosen using the GLCM method. Nevertheless, test results on paired regions were not completely satisfactory, specifically for LBP. Therefore, the critical pixel analysis is proposed to overcome the limitation due to ROI misalignment, yeilding resuls that disagree with gold standard only in two out of 16 cases. Now, let us focus our attention on these two cases: they are mixed edema, which cavities are filled by hemorrhagic corpusculated serum, with a high concentration of proteins and other strongly reflective elements. It is not a problem of reflectivity, because LBP is invariant to gray scale variations. Moreover, if thickness changes co-exist with texture variations, more (or less) numerous critical pixels should be found in a greater (or smaller) retinal area [17], under the reasonable hypothesis that the probability of a critical pixel remains constant. If so, however, variation in the mean retinal thickness will be proportonal to variation in the number of critical pixels; this is not true, just because critical pixels accumulate in pathological retinal regions, such as edema.

So, the proposed feature, the number of LBP based critical pixels, is a valid identifier of pathology severity and it allows to follow the evolution of the disease during its course and after therapy, with findings consistent with thickness measurement.

Similarly, the proposed shape index is able to quantify retinal morphology in a simple way, integrating also thickness analysis, though it is valid only if OCT images are centered on fovea.

Lastly, also segmentation errors must be taken into account in this work, as in pathological retinas it is difficult to discrimante between altered cellular layers, mainly in case of poor quality OCT images. Such difficulties are not completely overcome by automatic sofware system, e.g. [18].

As possible future developments of this work, we wold like to instance the use of critical pixels to segment edematous regions as well as the extension of LBP analysis to the 3D OCT images, now available.

In conclusion, even if our results should be confirmed on a wider image data set, quantitative analysis of retinal layers, as shown in OCT images, may represent a promising tool for improved monitoring of patients, earlier detection of pathology and more precise treatment protocols.

References

1. Age-Related Eye Disease Study Research Group, 2001. A randomized, placebo controlled, clinical trial of high-dose supplementation with vitamins C and E, betacarotene, and zinc for age-related macular degeneration and vision loss: AREDS report no. 8. Arch Ophthalmol 119, pp. 1417-1436.

2. Schuman JS, Puliafito C, Fujimoto JG. (2004) Optical coherence tomography of ocular diseases. 2nd ed. Thorofare, NJ.

3. Brezinski M. (2006) Optical Coherence Tomography: principles and applications. Academic Press, New York.

4. B. Lumbroso, M. Rispoli (2009) Guide to Interpreting Spectral Domain Optical Coherence Tomography. I.N.C.Innovation-News-Communication, Roma.

5. C. H. Chen, L. F. Pau, P. S. P. Wang, The Handbook of Pattern Recognition and Computer Vision (2nd Edition), 1998, pp. 207-248, World Scienti?c Publishing Co.

6. J. S. Weszka, C. R. Dyer, and A. Rosenfield (1976) A comparative study of texture measures for terrain classification. IEEE Trans. Syst., Man, Cybern., vol. SMC-6.

7. Manish H. Bharati, J. Jay Liu, John F. MacGregor, Image texture analysis: methods and comparisons, Elsevier, (2004), Ontario.

8. OjalaT., Pietikäinen M., MäenpääT. (2002) Multiresolution gray-scale and rotation invariant texture classi?cation with local binary patterns. IEEE Trans.Pattern Analysis and Machine Intelligence, 24: 971-987.

9. Heikkil M, Pietikainen M, Schmid C. Description of interest regions with local binary patterns. Pattern Recognition 42 (2009) 425-436.

10. Haralick R.M. (1979) Statistical and Structural Approaches to Texture. Proc.IEEE 67:786-804.

11. Cabrera Fernández D., Salinas H.M., Puliafito C.A. (2005) Automated detection of retinal layer structures on optical coherence tomography images. Opt. Express 13: 10200-216.

12. Baroni M., Fortunato P., La Torre A., Towards quantitative analysis of retinal features in Optical

Coherence Tomography, Medical Engineering& Physics , (2007), vol.29, pp.432-441.

13. Shahidi M., Wang Z., Zelkha R. (2005) Quantitative Thickness Measurement of Retinal Layers Imaged by Optical Coherence Tomography. Am J Ophthalmol 139:1056-61.

14. Schmitt JM, Xiang SH, Yung KM (1999) Speckle in optical coherence Tomography. J. Biomed. Optics 4: 95-100.

15. Narasimba-Iyer H, Can A, Roysam B, Stewart CV, Tanenbaum HL, Majerovics A, Singh H. Robust Detection and Classification of Longitudinal Changes in Color retinal fundus Images for Monitoring Diabetic Retinopathy. IEEE Trans Biomedical Engineering 53 (2006): 1084-1097.

16. Liu Y, Chen M, Ishikawa H, Wollstein G, Schuman JS, Rehg JM. Automated macular pathology diagnosis in retinal OCT images using multi-scale spatial pyramid and local binary patterns in texture and shape encoding. Medical Image Analysis 15 (2011) 748-759.

17. Jitendra Malik, Serge Belongie, Thomas Leung, Jianbo Shi. Contour and Texture Analysis for Image Segmentation, International Journal of Computer Vision, 43 (2001).

18. Koprowski R, Wróbel Z. Image Processing in Optical Coherence Tomography using Matlab. (2011) Published in Poland by University of Silesia, Institute of Computer Science, Department of Computer Biomedical Systems.

Acknowledgement

The authors wish to thank prof. Agostino La Torre, Department of Surgical Oto-Neuro-Ophthalmology Sciences, University of Florence, for his support with patient data and medical knowledge.

Illustrations

Illustration 1

top) OCT image of a normal eye; bottom) pathological OCT image of diabetic retinopathy with cystoid edema.

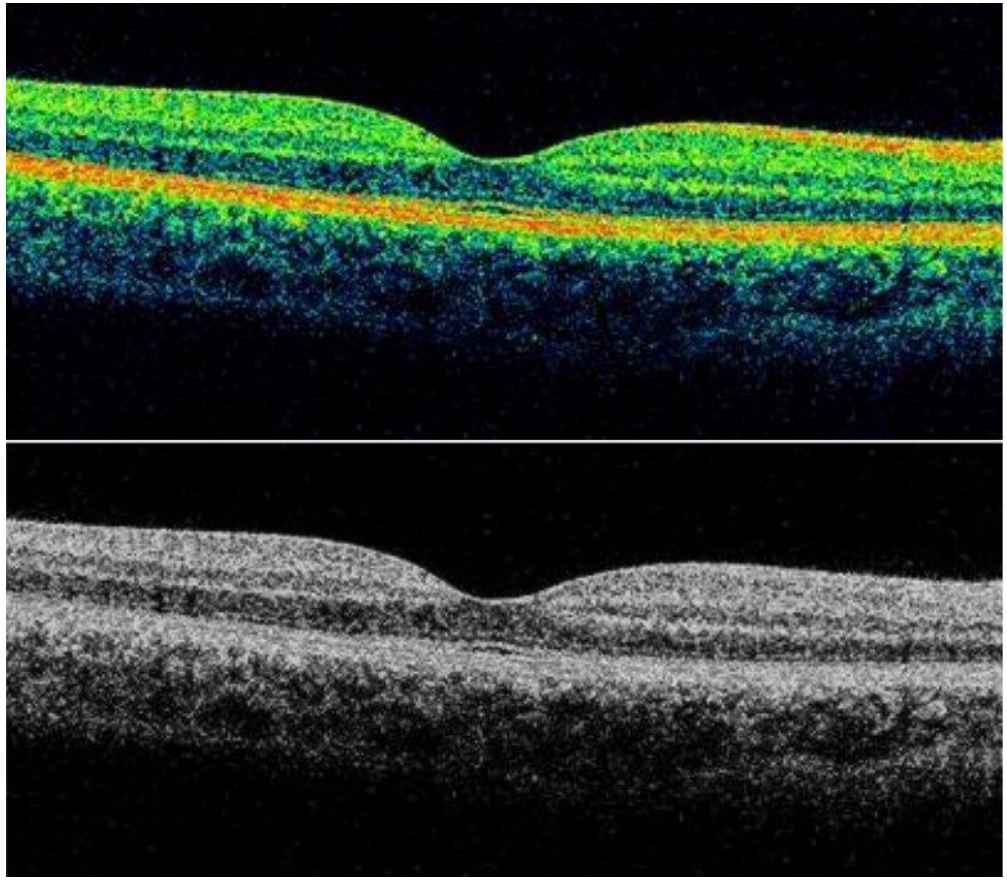

Illustration 2

Retinal cellular layers: A) a typical OCT scan; B) enlarged fovea; C) retinal tissue observed with optical miscroscopy; (bottom) a sketch of retina with layer terminology

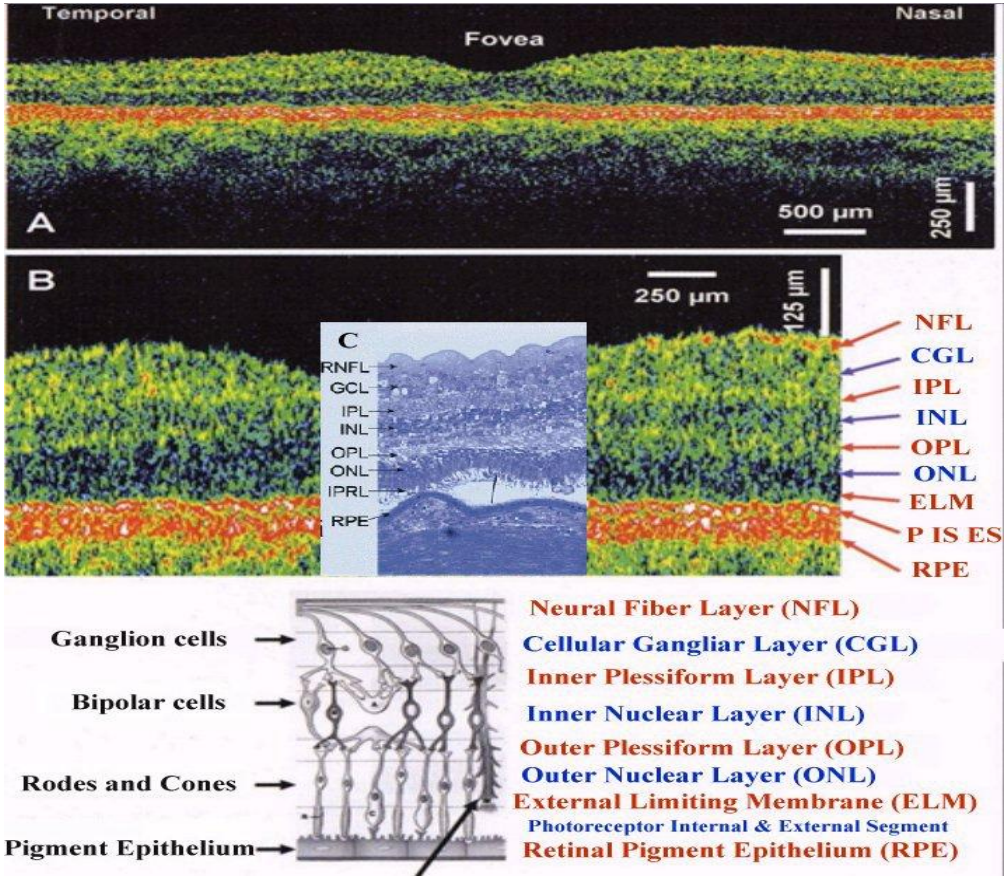

Illustration 3

OCT image with the three contours delimiting inner and outer (photoreceptor) layers, together with five ROI, delimited by green vertical lines.

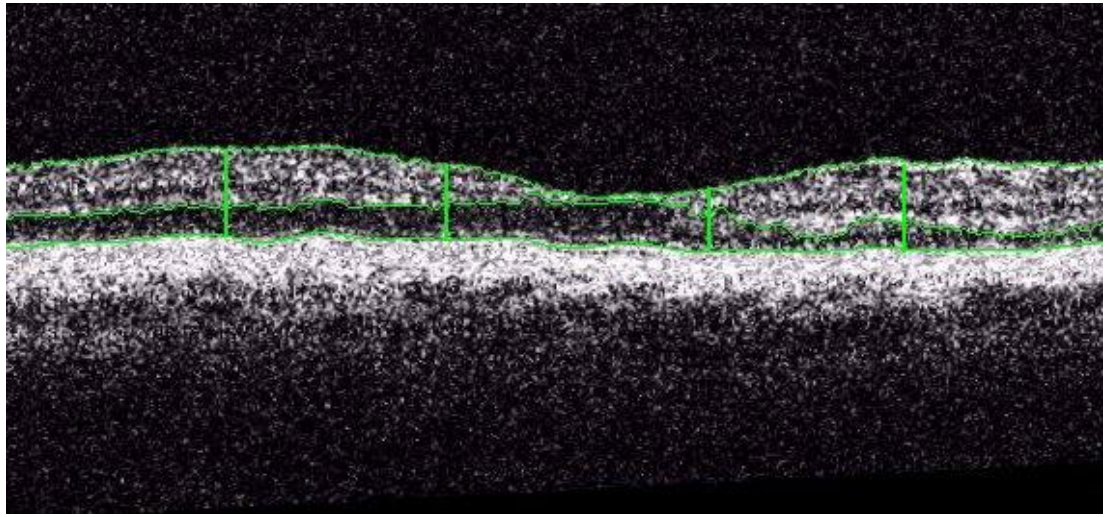

Illustration 4

Local Binary pattern: calculation for LBP code and local contrast.

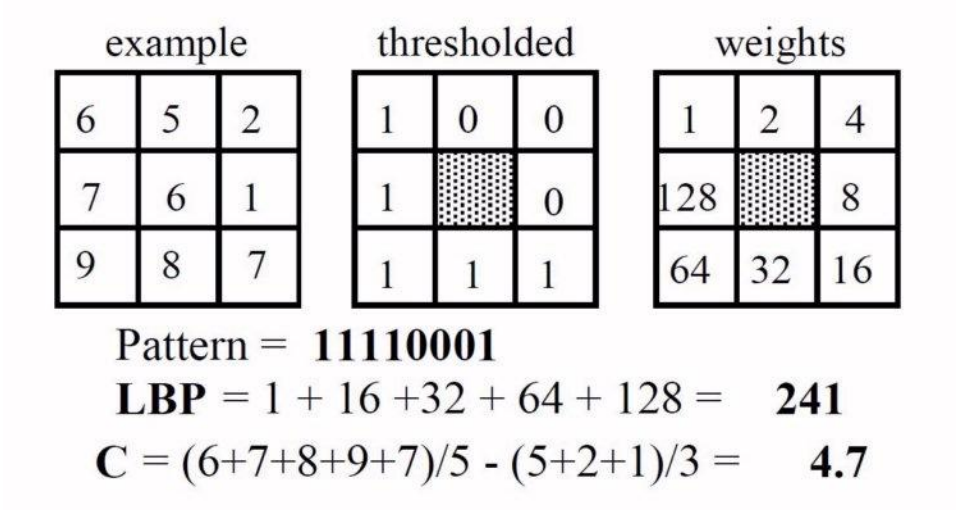

Illustration 5

Four examples of ROI for multiscale LBP calculation:
a) 3x3 , 7x5 b) 3x3 , 7x7   c) 5x5 , 7x7   d) 5x3 , 7x5 .

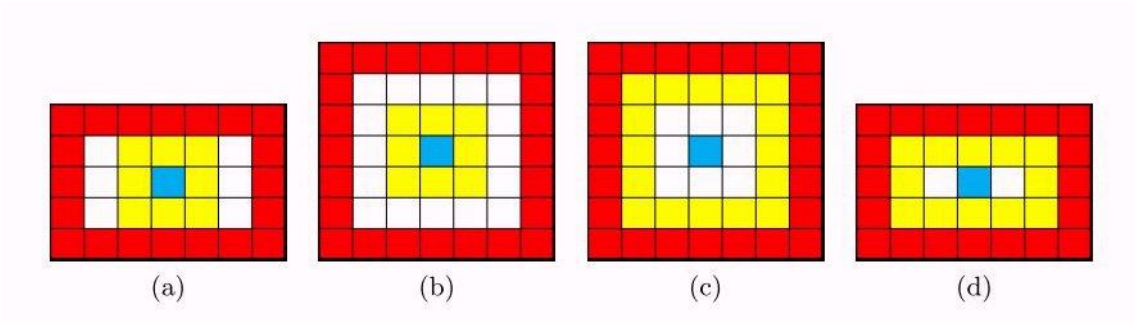

Illustration 6

Normal ranges of five texture parameters of GLCM (gray-level co-occurrence matrices) for each ROI covering full-thickness retina (see text for further explanations).
Results of the comparison with a pathological group is shown (significant differences are in yellow).

N=25 normals	Entropy	Contrast	Correlation	Energy	Homogeneity
ROI 1	1,34 ± 0,30	0,32 ± 0,19	0,84 ± 0,07	0,81 ± 0,04	0,95 ± 0,01
ROI 2	1,42 ± 0,22	0,36 ± 0,24	0,83 ± 0,07	0,79 ± 0,03	0,95 ± 0,01
ROI 3	1,03 ± 0,27	0,24 ± 0,18	0,79 ± 0,13	0,86 ± 0,05	0,97 ± 0,01
ROI 4	1,43 ± 0,34	0,36 ± 0.18	0,84 ± 0,12	0,79 ± 0,06	0,95 ± 0,01
ROI 5	1,26 ± 0,33	0,32 ± 0,15	0,84 ± 0,11	0,82 ± 0,06	0,96 ± 0,01
Full retina	1,296 ± 0,29	0,32 ± 0,19	0.828 ± 0.10	0.814 ± 0.048	0.956 ± 0.01
vs. 34 patients	p = 0.8 %	p = 55.6 %	p = 5.8 %	p = 0.6 %	p = 69.1 %
Accuracy(n=59)	94.9%	72.8%	91.5%	96.6%	66.1%

Illustration 7

Comparison between normal and pathological groups for LBP features, analysed in inner retina with 5x5 neighborouhoods and np=16 (significant differences are shown in yellow).

Inner Retina	LBP code	LBP contrast
25 normals	53,66 ± 2.41	62,41 ± 2.71
34 patients	57,46 ± 3.52	61,29 ± 4.14
p	1.02 % < 5 %	42.55 %

Illustration 8

Comparison between normal and pathological groups for multriscale LBP, analysed in inner retina, with 3x3 and 7x7 neighborouhoods and np=8 (significant differences are shown in yellow).

multi scale LBP inner retina	3x3 7x5	3x3 7x7	5x5 7x7	5x3 7x5
25 normals	87.40 ± 4.49	84.56 ± 4.36	87.92 ± 3.31	90.27 ± 3.47
34 patients	91.12 ± 5.73	114.49 ± 29.46	92.98 ± 5.09	94.13 ± 4.82
p	0,93%	0,0005%	0,0061%	0,124%

Illustration 9

Follow-up of 16 retinal OCT: results by GLCM (normal range and t-test), LBP (Dc%, i.e. difference in critical pixel number) and thickness analyses (difference in fovea shape index, DIt%, and in retina thickness, Dt%) wrt qualitative evaluation of edema and fovea morphology. Equal signs (=) mean no changes detected between pre and post images; plus sign (+) indicates an improvement, minus sign (-) indicates worsening; asterisks mean disagreement wrt gold standard.

Case	GLCM Normal range	GLCM p%	Δc%	ΔIt%	Δt%	edema	fovea
1	=	7.3	-11.7 *	1.0	-5.6	=	=
2	+	2.2	17.5	25.7	17.9	+	+
3	+*	4.8	-4.3	4.5	4.9	-	+
4	-*	2.6 *	2.4	-24.7	1.1	=	-
5	-	3.0	-56.3	-7.1	-26.4	-	-
6	+	4.9	5.4	0.09	5.0	+	=
7	+	6.8 *	-11.8 *	3.6	1.0 *	+	=
8	+	5.1	8.4	6.8	11.1	+	+
9	+	2.1	19.7	28.9	13.0	+	+
10	-	7.4 *	-49.9	-64.2	-28.8	-	-
11	=*	3.9	-35.1	-45.2	-7.7	-	-
12	-	2.8	-52.3	-4.1	-12.9	-	-
13	+	4.1	36.9	7.7	30.8	+	+
14	-	2.5	-14.5	33.7	-6.8	-	+
15	+	4.2	21.0	3.4	9.6	+	=
16	=*	1.8	38.9	8.0 *	11.2	+	=
accuracy	75%	81.25%	87.5%	93.75%	93.75%	gold standard	

Illustration 10

Follow-up of a pathological retina (included within two green contours) with an improved cystoid edema. Pre-treatment image is shown above, post-treatment image is below. LBP based critical pixels are shown in red (see text for explanations).

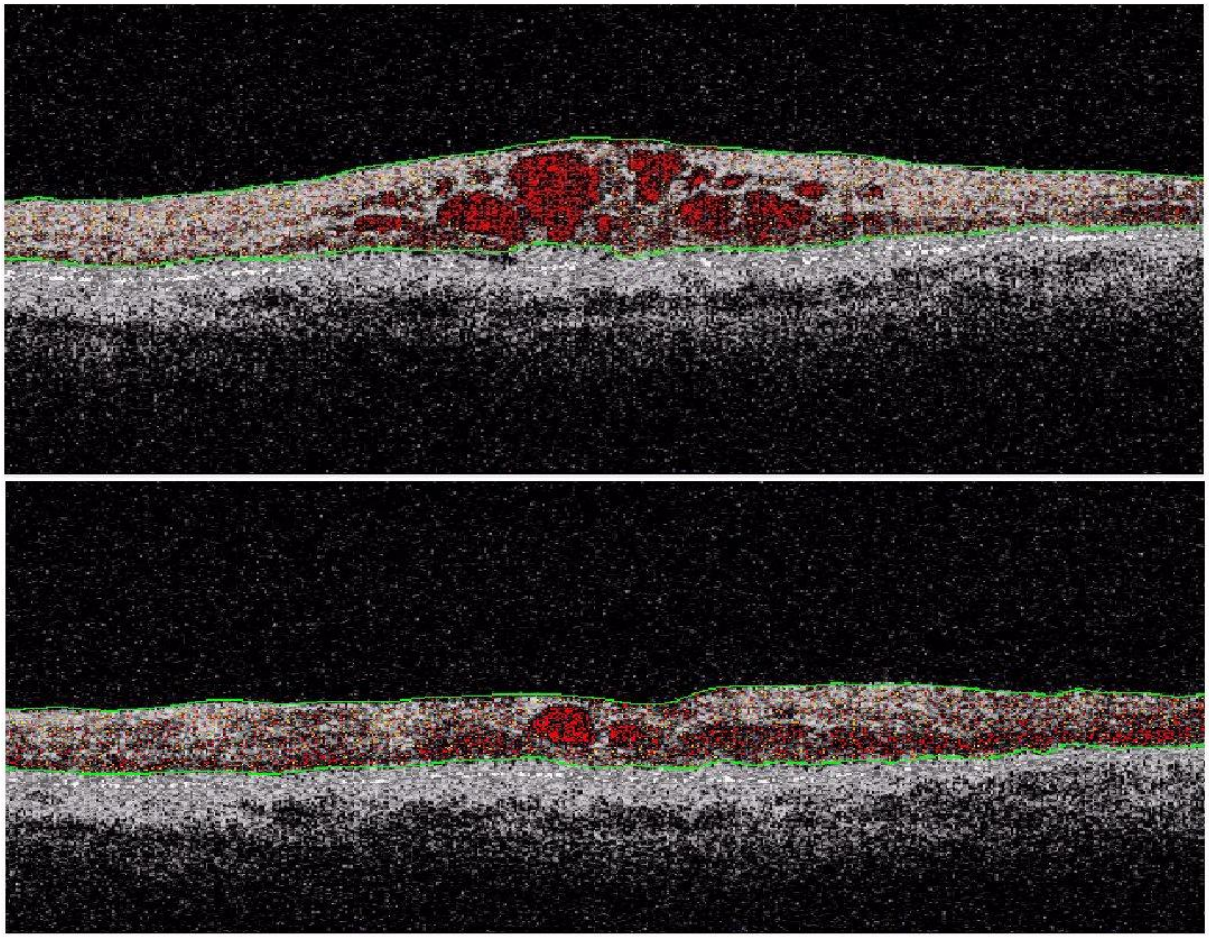

Illustration 11

Follow-up of a pathological retina (included within two green contours) with nearly stationary conditions. Pre-treatment image is shown above, post-treatment image is below. LBP based critical pixels are shown in red (see text for explanations).